Competition between zero-phonon and phonon-assisted luminescence in colloidal CdSe quantum dots

F. J. P. Wijnen,[1] J. H. Blokland,[1] P. T. K. Chin,[2] P. C. M. Christianen,[1,*] and J. C. Maan[1]

[1]*High Field Magnet Laboratory, Institute for Molecules and Materials, Radboud University Nijmegen, Toernooiveld 7,*
6525 ED Nijmegen, The Netherlands

[2]*Molecular Materials and Nanosystems, Eindhoven University of Technology, P.O. Box 513, 5600 MB Eindhoven, The Netherlands*

We determine the low-temperature optical properties of dark-exciton states in CdSe/CdS nanocrystal quantum dots (NQDs). By using *resonant* laser excitation we distinguish zero-phonon from phonon-assisted photoluminescence. The NQDs show a decreasing zero-phonon intensity with decreasing temperature, resulting in a redshift of the *nonresonant* photoluminescence. This redshift is undone by application of a magnetic field. Our results show that dark-exciton luminescence originates from the intricate competition of phonon-assisted and zero-phonon transitions, the latter of which are enhanced by dark–bright-exciton mixing due to unpassivated surface states or a magnetic field.

PACS number(s): 78.67.Hc, 78.55.−m, 71.35.−y

Colloidal semiconductor nanocrystal quantum dots (NQDs) have remarkable optical properties, such as widely tunable emission wavelengths[1] and high quantum efficiencies at room temperature.[2] Due to these properties and the relatively easy fabrication method, NQDs are very promising for a broad range of applications.[3–9] Surprisingly, the origin of the NQD optical transitions at low temperatures is still not clear,[10–13] in particular because the lowest-energy transition is associated with a dark-exciton state, i.e., an optically forbidden transition.[14,15] The purpose of this work is to investigate the recombination mechanisms of dark excitons by reporting a detailed photoluminescence (PL) study of core/shell CdSe/CdS NQDs as a function of temperature, magnetic field, and shell thickness.

Three-dimensional confinement of electrons and holes in semiconductor NQDs leads to a discrete atomlike level structure. It is well established that in wurtzite NQDs the electron-hole exchange interaction and the intrinsic crystal/shape anisotropy lift the spin degeneracy of the exciton levels, leading to five distinct states, characterized by their spin projection F along the NQD c axis.[15,16] Evidence for this exciton fine structure has been given by the size-dependent Stokes shift from fluorescence line narrowing[15,17] (FLN), and the dependence of the radiative lifetime on temperature[10,18] and magnetic fields.[14,19] To understand the low-temperature optical properties, only the two lowest twofold-degenerate levels are important, which are lower-(higher-)energy exciton levels with $F = \pm 2$ ($F = \pm 1^L$) that are dipole forbidden (allowed). The separation between the two levels is given by the exchange splitting (Δ_{bd}) which depends on NQD size. For typical values of Δ_{bd} of 5–20 meV, only the lowest $|F| = 2$ level is populated at low temperatures (<10 K). The radiative lifetime of this level has been found to be remarkably short for a dark state (~ 1 μs).[10] This apparent brightness has been attributed to phonon-assisted transitions,[14] supported by a redshift of the PL energy with decreasing temperature when the lower-energy phonon replicas gain importance relative to the zero-phonon line.[20] Alternatively, the bright zero-phonon emission has been suggested to be due to mixing of the dark- and bright-exciton states, for instance as

a result of unpassivated surface sites.[11,21] Furthermore, it has been shown that a magnetic field mixes the dark- and bright-exciton levels and thereby decreases the radiative lifetime of the zero-phonon line, making its contribution to the total PL emission larger with respect to the phonon-assisted transitions.[14,15,19] A magnetic field is thus a powerful tool in studying the interplay between the different phonon-assisted and zero-phonon lines.

To investigate the nature of the dark-exciton emission of wurtzite NQDs, we performed a detailed PL study, which includes temperature-dependent, resonant, and nonresonant PL spectroscopies in high magnetic fields (B) up to 33 T. Experiments with *resonant* laser excitation allowed us to determine the relative importance of zero-phonon and phonon-assisted transitions and connect changes therein to energy shifts observed in *nonresonant* experiments. We show that variation in temperature, magnetic field, and NQD shell thickness can shift the subtle balance between these recombination processes in either direction.

The samples were prepared by drop casting a solution of core/shell CdSe/CdS NQDs (Ref. 22) in toluene on fused silica. The CdSe core has a radius of 17.8 Å, and is either uncoated (QD0) or it is coated by a single (QD1) or triple (QD2) monolayer (ML) shell of CdS. The NQDs were capped with tri-*n*-octylphosphine (TOP), tri-*n*-octylphosphine oxide (TOPO), and hexadecylamine (HDA). The samples were mounted in Faraday geometry inside a liquid-helium bath cryostat in a 33 T Bitter-type electromagnet and cooled to 1.2–4.2 K. We measured PL of the NQDs using both nonresonant and resonant laser excitations. The nonresonant PL was excited by 2.7 eV laser light, dispersed by a single grating spectrometer, and detected by a liquid nitrogen cooled charge-coupled device (CCD) camera in 30 s exposures. For the QD1 experiments both circular polarizations were obtained simultaneously by inserting a polarizing beam splitter in the detection path.[23,24] The two circular polarizations of the QD0 and QD2 PL were recorded in two consecutive sweeps with opposite current directions through the magnet.

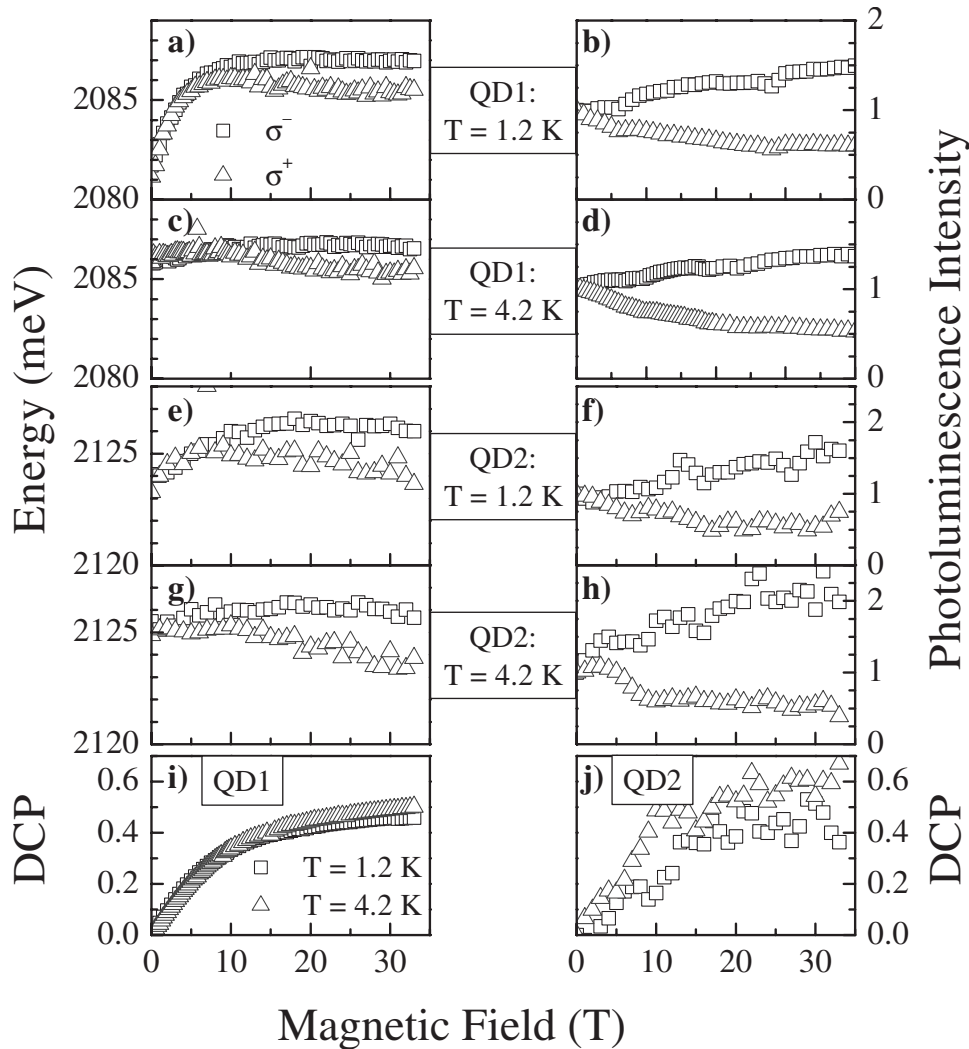The NQDs show asymmetric PL spectra with a full width

FIG. 1. Top panel: peak energy (left) and integrated intensity (right) of the nonresonant photoluminescence of two types of quantum dots at different temperatures. The integrated PL intensities are normalized to their values at zero field. The squares (triangles) correspond to σ^- (σ^+) polarized energies and intensities. Bottom panel: DCP for both dots. The squares (triangles) correspond to 1.2 (4.2) K.

at half maximum of 85 meV. The spectrum was fitted by a single Gaussian to obtain the peak energy. Figure 1 shows the peak energy (a,c,e,g), integrated intensity (b,d,f,h), and the degree of circular polarization (DCP) $[=(I_{\sigma^-}-I_{\sigma^+})/(I_{\sigma^-}+I_{\sigma^+}),i,j]$ as function of B at 1.2 and 4.2 K for QD1 and QD2. We recognize the following trends: at $B=0$ T the PL energy is lower at 1.2 K than at 4.2 K, namely, ~4 meV for QD1 [Figs. 1(a) and 1(c)], and ~2 meV for QD0 (not shown) and QD2 [Figs. 1(e) and 1(g)]. This redshift at 1.2 K is undone by a magnetic field of ~10 T [Figs. 1(a) and 1(e)]. With increasing B the PL becomes circularly polarized, where the σ^- emission shifts to higher energy with increasing intensity and the σ^+ emission shifts to lower energy with decreasing intensity. The corresponding DCP equals 0.5–0.6 at $B=33$ T, and only slightly depends on temperature [Figs. 1(i) and 1(j)].[19,25] Remarkably, we measured the highest intensity at the highest energy for both temperatures, similar to an earlier report.[19] Finally, for all samples the total normalized PL intensity only marginally increases with B from 2 ($B=0$ T) to 2.4 at $B=33$ T.

To determine the contributions of different recombination

mechanisms, PL was measured under resonant excitation (FLN).[14] The sample was mounted on a fiber coupled probe,[24] and resonantly excited by a tunable dye laser using circularly polarized light. Excitation and detection occurred under crossed polarization to minimize scattered laser light. Spectra were recorded in 60 s exposures.

Typical FLN spectra are shown in Fig. 2(a) and can be roughly understood in terms of the exciton level scheme in Fig. 2(c). Excitons are excited by the laser into the bright $F=\pm1^L$ levels, resulting in emission from the dark $F=\pm2$ excitons, i.e., the zero-phonon line (ZPL) 6 meV below the laser energy, and several phonon replicas (1PL, 2PL), superimposed on a small nonresonant PL background. The energy positions and intensities of all resolved peaks were obtained by fitting a Lorentzian laser line and Gaussian peaks for the ZPL, 1PL, and 2PL, and the nonresonant background. Figure 2(b) shows the ZPL and 1PL intensities as a function of temperature, relative to the ZPL intensity at 4.2 K (QD2). The ZPL intensity steadily decreases with decreasing temperature, whereas the 1PL intensity slightly increases,[20] a
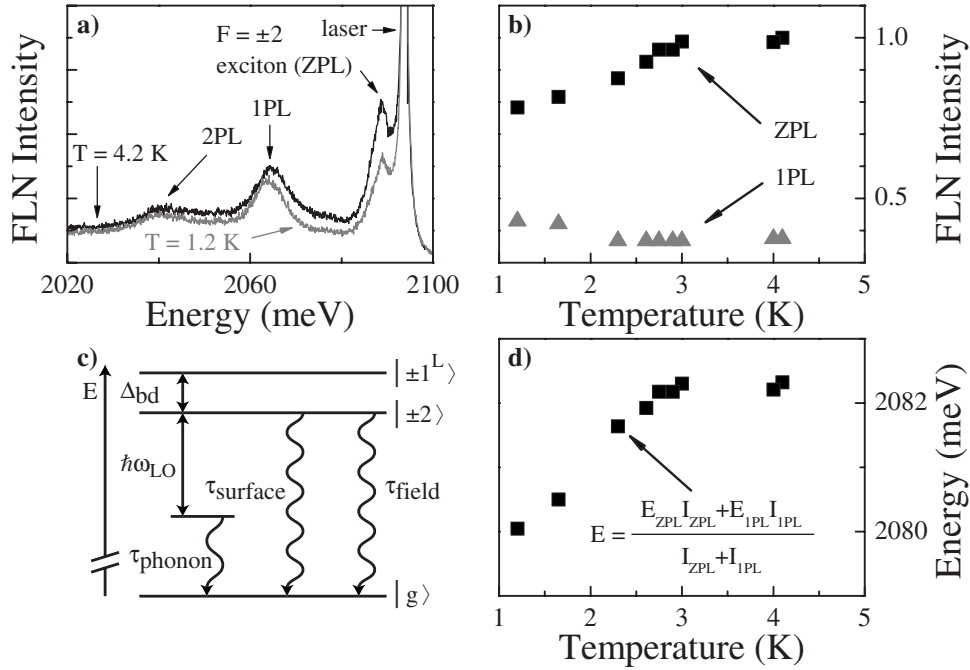
FIG. 2. (a) FLN spectra of QD2 at 4.2 (black line) and 1.2 K (gray line) that show the dark $F = \pm 2$ exciton (ZPL) emission and two phonon replicas (1PL, 2PL). (b) Temperature dependence of the ZPL (black squares) and 1PL (gray triangles) intensities relative to the ZPL intensity at 4.2 K. (c) Schematic representation of the lowest excitonic states and three possible recombination processes explained in the text. The dark state $F = \pm 2$ and bright $F = \pm 1^L$ exciton are separated in energy by Δ_{bd}, and $\hbar\omega_{LO}$ is the LO phonon energy. Zeeman splitting due to a magnetic field has been omitted for clarity. (d) The temperature dependence of the intensity weighted average energy of the ZPL and 1PL.

trend that is also directly visible in the FLN spectra [Fig. 2(a)].

Figure 3(a) shows the evolution of the FLN spectrum with increasing B at 1.2 K, using σ^+ polarized excitation and detecting σ^- polarized PL. The ZPL shifts to lower energy due to the Zeeman splitting and becomes more intense with field. At high fields (>15 T) an additional peak appears between the laser and the ZPL. This peak has been reported previously[24] and is due to resonant σ^+ polarized excitation into the $+1^L$ state and subsequent σ^- polarized emission of -1^L excitons after a spin-flip process. The measured splitting increases linearly with B and is directly related to the Zeeman splitting of the $F = \pm 1^L$ levels. The observation of this line is further evidence for the exciton fine-structure model.[24] Figure 3(b) plots the fitted ZPL and 1PL intensities as a function of B. The ZPL intensity increases considerably, in particular at 1.2 K where a threefold enhancement is observed. In contrast, the intensity of the phonon replica is almost constant (open diamonds).

To describe the data we consider the different recombination channels of neutral excitons that are schematically shown in Fig. 2(c), taking into account bright $F = \pm 1^L$ and dark $F = \pm 2$ levels. Note that for sake of clarity the Zeeman splittings of the exciton lines have been omitted in this figure. Given the measured exchange splitting Δ_{bd} of ~ 6 meV, the $F = \pm 1^L$ levels are not populated at the low temperatures used here. Therefore, we only need to include recombination from the $F = \pm 2$ levels, where we distinguish three recombination processes: surface-state assisted transitions,[11] phonon-assisted transitions,[13,14] and direct zero-phonon transitions.

The optical phonon-assisted 1PL lies typically $\hbar\omega_{LO} = 25-26$ meV below the $F = \pm 2$ level [Fig. 2(a)],[17] and is characterized by the recombination lifetime τ_{phonon}. Direct recombination of the dark excitons can only occur through mixing with the bright excitons, either due to a magnetic field (τ_{field}) (Refs. 14, 15, 19, and 25) or due to unpassivated surface states ($\tau_{surface}$).[11] Clearly, this schematic model ignores recombination of charged excitons or biexcitons, as well as the chemical details of the actual states at the NQD surface, which might lead to modifications of the exciton fine structure and the optical recombination.[11,21] Within the experimental resolution of our FLN experiment, however, we did not find any deviations from this simple level scheme.

The actual dark-exciton recombination is governed by the competition between the different transitions, depending on temperature, magnetic field, and surface passivation. Let us first consider the temperature dependence of the NQD emission. In the FLN experiment we observed a reduced ZPL emission with decreasing temperature, whereas the intensity of the phonon replicas only marginally increases [Fig. 2(b)]. This redistribution among the ZPL and 1PL lines[20] is responsible for the temperature dependence of the nonresonant PL. The nonresonant spectrum is the averaged PL emission of an ensemble of NQDs with slightly different sizes. For typical size variations of about 5%, the ensemble PL linewidth is larger than the LO phonon energy, which implies that the nonresonant PL spectrum is an average of nonphonon and phonon-assisted lines. We simulate this average PL by combining the extracted energies and intensities of the ZPL and 1PL emissions in the FLN spectra [Fig. 2(b)] to calculate the
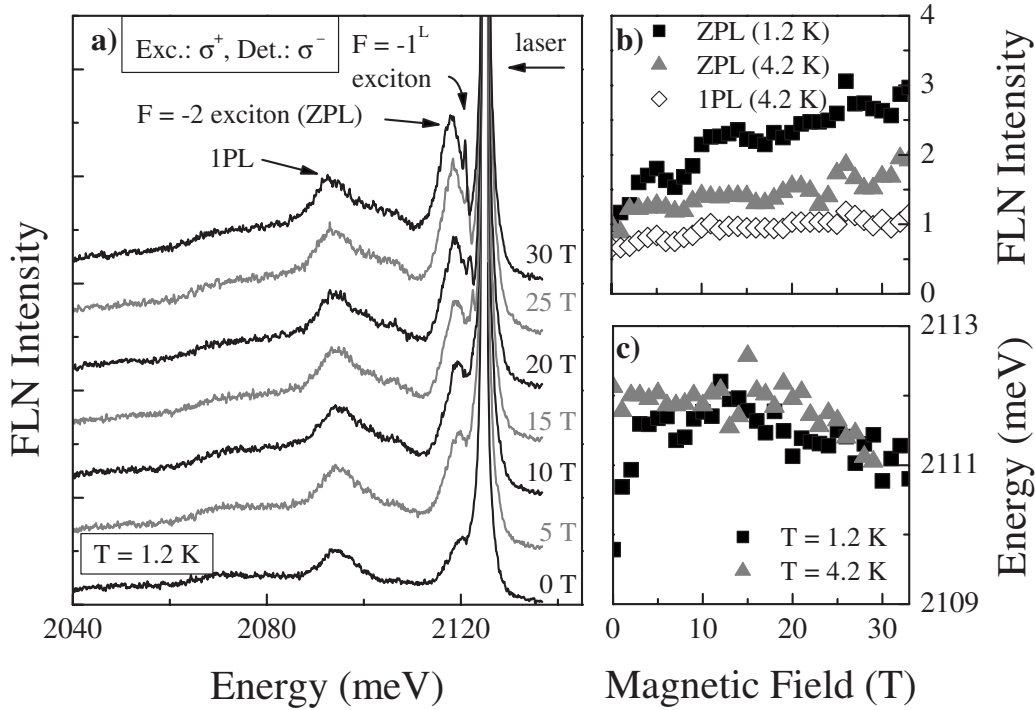
FIG. 3. (a) FLN spectra of QD2 with increasing magnetic field at 1.2 K with σ^+ polarized excitation and σ^- detection. (b) The intensity of the ZPL emission at 1.2 (squares) and 4.2 K (triangles), and the 1PL intensity at 4.2 K (open diamonds) as a function of magnetic field. (c) The intensity weighted average energy position as a function of magnetic field at 1.2 K (4.2 K), squares (triangles).

intensity weighted average energy position [Fig. 2(d)]. We find a shift of approximately 2 meV toward lower energy, from 2082 meV at 4.2 K to 2080 meV at 1.2 K, which matches remarkably well with the observed redshift of the nonresonant PL line of QD2 upon cooling [Figs. 1(e) and 1(g)]. This observation indicates that the redshift is related to a decreasing ZPL intensity compared to the phonon replica at lower energy.

The size of the redshift, i.e., the ratio between ZPL and 1PL emissions, is sample dependent (4 meV for QD1, and 2 meV for QD0 and QD2), which is most probably due to the different surface-state assisted recombination of the different NQD samples caused by the difference in shell thickness. Overcoating the NQD core with an inorganic shell decreases the influence of unpassivated surface states on the optical emission, leading to an increased quantum yield with an optimum at a certain shell thickness ($\sim 1-2$ ML).[26,27] A reduced surface-state assisted emission results in a diminished ZPL emission (τ_{surface} becomes longer). Changing the shell thickness thus changes the relative importance of the ZPL and phonon-assisted emission, leading to a sample-dependent redshift upon cooling, which also explains the wide range of values, up to 13 meV,[10] reported in literature.

The competition between zero-phonon and phonon-assisted recombination is further supported by the results in high magnetic fields. A magnetic field has several effects on the exciton levels. First, the field causes the mixing of dark with bright excitons.[14,15] The strength of the mixing depends on the angle of the NQD c axis with respect to the direction of B. On average it will lead to an enhanced ZPL intensity compared to the phonon replica emission [Figs. 3(b) and 3(c)].[14,24] Calculating the intensity weighted average energy

position of the ZPL and 1PL [see Fig. 3(c)], we find that at 1.2 K the average energy shifts 2 meV upward from 2110 (0 T) to 2112 meV at 10 T. This behavior matches very well with the observed shifts in the nonresonant PL experiment [compare with Figs. 1(e) and 1(g)]: the redshift upon cooling is canceled by application of a magnetic field of 10 T.

The second important effect of B is the Zeeman splitting of the exciton levels, which is visible in the FLN data as an increasing separation between the laser line and the $F=-2$ and $F=-1^L$ emission with growing field [Fig. 3(a)]. Furthermore, as a result of the Zeeman effect, we observed an energy separation of ~ 1 meV at $B=33$ T, between the σ^- and σ^+ polarizations, and a profound DCP [Figs. 1(i) and 1(j)]. The B dependence of the DCP appears to be described well within the exciton fine-structure model, a fact that was repeatedly used to support this model.[19,25] However, with the parameters used to fit the DCP, the model fails to describe three other characteristic features: (i) the peculiar polarization of the PL emission, i.e., that the highest energy has the highest intensity, (ii) the actual value of the observed energy splitting (Fig. 1), and (iii) the nonzero intensity of the low-temperature PL. Therefore, we find that the exciton fine-structure model cannot fully describe the high magnetic-field experiments, which confirm that a complete description of the dark-exciton PL should include multiple recombination channels.

A complete theory for dark-exciton recombination that is capable of explaining all experimental observations is still lacking. Therefore, we propose the schematic dark-exciton recombination scheme of Fig. 2(c), which combines ingredients from several different theoretical descriptions. The starting point is an exciton fine structure, in which bright- and

dark-exciton levels are split due to exchange interactions. This fine structure has been calculated by either an effective-mass approximation model[15] or atomistic pseudopotential calculations.[11] To explain the finite lifetime of the dark-exciton ground state, mixing of bright and dark excitons is needed, for instance due to unpassivated surface states.[11] This lifetime, however, is still very long ($\sim \mu$s) and therefore phonon-assisted transitions should also be taken into account.[13,17,20] The competition between these direct and phonon-assisted transitions explains the redshift of the dark-exciton emission upon cooling from 4.2 to 1.2 K and the cancellation of this redshift by a magnetic field. This magnetic-field effect is due to the mixing of the dark- and bright-exciton states, as described by the effective-mass model.[15] Although this model describes the enhancement of the ZPL intensity in a magnetic field, it fails to explain the observed splitting of σ^- and σ^+ polarized PL, and the peculiar PL polarization. This confirms the crucial role of phonon-assisted and surface-state assisted recombination channels.

In conclusion, we have found that the low-temperature dark-exciton emission of CdSe/CdS NQDs is determined by the competition between phonon-assisted and zero-phonon recombination. The relative importance of the different recombination processes depends strongly on internal factors, such as shell thickness and surface passivation, and on external factors, such as temperature and a magnetic field. Our results prove that any model that attempts to fully describe the optical properties of CdSe NQDs should include, besides the exciton fine structure, also phonon-assisted and surface-state assisted recombinations.

*Corresponding author.

[1] A. P. Alivisatos, Science **271**, 933 (1996).

[2] L. Qu and X. Peng, J. Am. Chem. Soc. **124**, 2049 (2002).

[3] M. Bruchez Jr., M. Moronne, P. Gin, S. Weiss, and A. P. Alivisatos, Science **281**, 2013 (1998).

[4] A. R. Clapp, I. L. Medintz, J. M. Mauro, B. R. Fisher, M. G. Bawendi, and H. Mattoussi, J. Am. Chem. Soc. **126**, 301 (2004).

[5] V. L. Colvin, M. C. Schlamp, and A. P. Alivisatos, Nature (London) **370**, 354 (1994).

[6] S. Coe, W.-K. Woo, M. Bawendi, and V. Bulovic, Nature (London) **420**, 800 (2002).

[7] N. Tessler, V. Medvedev, M. Kazes, S. Kan, and U. Banin, Science **295**, 1506 (2002).

[8] M. Achermann, M. A. Petruska, S. Kos, D. L. Smith, D. D. Koleske, and V. I. Klimov, Nature (London) **429**, 642 (2004).

[9] V. I. Klimov, A. A. Mikhailovsky, S. Xu, A. Malko, J. A. Hollingsworth, C. A. Leatherdale, H. J. Eisler, and M. G. Bawendi, Science **290**, 314 (2000).

[10] S. Crooker, T. Barrick, J. Hollingsworth, and V. Klimov, Appl. Phys. Lett. **82**, 2793 (2003).

[11] M. Califano, A. Franceschetti, and A. Zunger, Nano Lett. **5**, 2360 (2005).

[12] C. de Mello Donega, M. Bode, and A. Meijerink, Phys. Rev. B **74**, 085320 (2006).

[13] T. J. Liptay, L. F. Marshall, P. S. Rao, R. J. Ram, and M. G. Bawendi, Phys. Rev. B **76**, 155314 (2007).

[14] M. Nirmal, D. J. Norris, M. Kuno, M. G. Bawendi, A. L. Efros, and M. Rosen, Phys. Rev. Lett. **75**, 3728 (1995).

[15] A. L. Efros, M. Rosen, M. Kuno, M. Nirmal, D. J. Norris, and M. Bawendi, Phys. Rev. B **54**, 4843 (1996).

[16] A. L. Efros and M. Rosen, Annu. Rev. Mater. Sci. **30**, 475 (2000).

[17] D. J. Norris, A. L. Efros, M. Rosen, and M. G. Bawendi, Phys. Rev. B **53**, 16347 (1996).

[18] O. Labeau, P. Tamarat, and B. Lounis, Phys. Rev. Lett. **90**, 257404 (2003).

[19] M. Furis, J. A. Hollingsworth, V. I. Klimov, and S. A. Crooker, J. Phys. Chem. B **109**, 15332 (2005).

[20] M. Nirmal, C. B. Murray, and M. G. Bawendi, Phys. Rev. B **50**, 2293 (1994).

[21] M. Califano, A. Franceschetti, and A. Zunger, Phys. Rev. B **75**, 115401 (2007).

[22] P. Chin, R. Hikmet, S. Meskers, and R. Janssen, Adv. Funct. Mater. **17**, 3829 (2007).

[23] T. Ha, T. Laurence, D. Chemla, and S. Weiss, J. Phys. Chem. B **103**, 6839 (1999).

[24] M. Furis, H. Htoon, M. A. Petruska, V. I. Klimov, T. Barrick, and S. A. Crooker, Phys. Rev. B **73**, 241313(R) (2006).

[25] E. Johnston-Halperin, D. D. Awschalom, S. A. Crooker, A. L. Efros, M. Rosen, X. Peng, and A. P. Alivisatos, Phys. Rev. B **63**, 205309 (2001).

[26] B. O. Dabbousi, J. Rodriguez-Viejo, F. V. Mikulec, J. R. Heine, H. Mattoussi, R. Ober, K. F. Jensen, and M. G. Bawendi, J. Phys. Chem. B **101**, 9463 (1997).

[27] X. Peng, M. C. Schlamp, A. V. Kadavanich, and A. P. Alivisatos, J. Am. Chem. Soc. **119**, 7019 (1997).